Highly selective catalysts for liquid-phase hydrogenation of substituted alkynes based on Pd—Cu bimetallic nanoparticles

*I. S. Mashkovsky,[a] P. V. Markov,[a] G. O. Bragina,[a] O. P. Tkachenko,[a] I. A. Yakushev,[b] N. Yu. Kozitsyna,[b] M. N. Vargaftik,[b] and A. Yu. Stakheev[a]**

[a]*N. D. Zelinsky Institute of Organic Chemistry, Russian Academy of Sciences, 47 Leninsky prosp., 119991 Moscow, Russian Federation. E-mail: st@ioc.ac.ru*

[b]*N. S. Kurnakov Institute of General and Inorganic Chemistry, Russian Academy of Sciences, 31 Leninsky prosp., 119991 Moscow, Russian Federation.*

Catalytic properties of Pd—Cu bimetallic catalysts supported on SiO_2 and Al_2O_3 were studied in a model reaction of selective hydrogenation of diphenylacetylene. Application of $PdCu_2(AcO)_6$ heterobimetallic acetate complex as a precursor made it possible to obtain homogeneous Pd—Cu bimetallic nanoparticles. This result was supported by the data of IR spectroscopy of adsorbed CO. The Pd-Cu catalysts showed considerably higher selectivity than monometallic samples. Moreover, the introduction of copper decreases the hydrogenation rate of diphenylethylene (DPE) to diphenylethane. As a result, the maximum yield of the target product, DPE, increased from 78 to 93% in the presence of Pd—Cu catalysts.

Key words: bimetallic catalysts, Pd, Cu, hydrogenation, alkynes, diphenylacetylene.

The selective catalytic hydrogenation of alkynes is one of the most important reactions since it serves to produce cis- and trans-alkenes which could be used as building blocks on different stages of fine organic synthesis.[1—3] Pd-supported catalysts characterized by a high hydrogenation activity are commonly used in selective hydrogenation reactions. However, a high rate of the hydrogenation of target alkene to alkane decreases the selectivity of the process.[4]

At present, a commercial Lindlar catalyst (Pd(5%)—$PbO/CaCO_3$) is widely applied for the cis-alkene synthesis from alkynes. Despite its high selectivity, an essential disadvantage is the presence of toxic lead compounds in its structure which are required for a partial deactivation of the catalyst to avoid overhydrogenation and alkane formation. Moreover, the catalyst can not be used for hydrogenation of a number of substrates (therminal alkynes as an example)[2] and it is not always stable under the reaction conditions.[5]

An efficient approach for development of a selective catalyst for C≡C bond hydrogenation involves using bimetallic Pd—M compositions, where M = Ag, Zn, Cu, *etc*.[6] According to the literature, modification of Pd catalysts with silver[7,8], zinc[9,10], gold[11,12] or copper [13,14] provides an improved selectivity in alkene formation. A special interest evoke bimetallic Pd—Cu complexes, because modification with copper increases the selectivity both in gas phase and liquid phase reactions.[13—15]

However, to prepare a highly selective catalyst, homogeneous bimetallic particles which do not contain Pd^0 need to be formed on the support surface. Such particle formation is not always achieved when traditional catalyst preparation methods are used. At the same time application of heterobimetallic acetate complexes of palladium with a second metal as precursor is one of the most effective technique to prepare highly homogeneous bimetallic catalyst.[9,16,17] In such complexes atoms of the both metals are strongly bounded by acetate bridges that allow them to keep the intimate contact on every step of the preparation and activation of the catalyst providing bimetallic nanoparticle formation in the final catalyst.[16,17]. In the present work, an approach referred to above was applied for preparing Pd—Cu catalyst for the liquid phase selective hydrogenation of substituted alkynes. In order to determine the influence of the support on catalytic properties and structure, silica (SiO_2) and alumina (Al_2O_3) were used to prepare both mono- and bimetallic samples. Catalytic characteristics of these systems were investigated in a model reaction of diphenylacetylene (DPA) hydrogenation.

The selective hydrogenation of the substituted alkynes operates in two steps (Scheme 1). At the first step, alkyne hydrogenates mainly to alkene, while at the second step the formed alkene hydrogenates to alkane which is undesirable process. Therefore it is necessary to minimize the rate of the second reaction step. So the hydrogenation rate ratio at the first and the second steps is an impor-

Published in Russian in *Izvestiya Akademii Nauk. Seriya Khimicheskaya,* No. 2, pp. 0425—0431, February, 2016.

Scheme 1

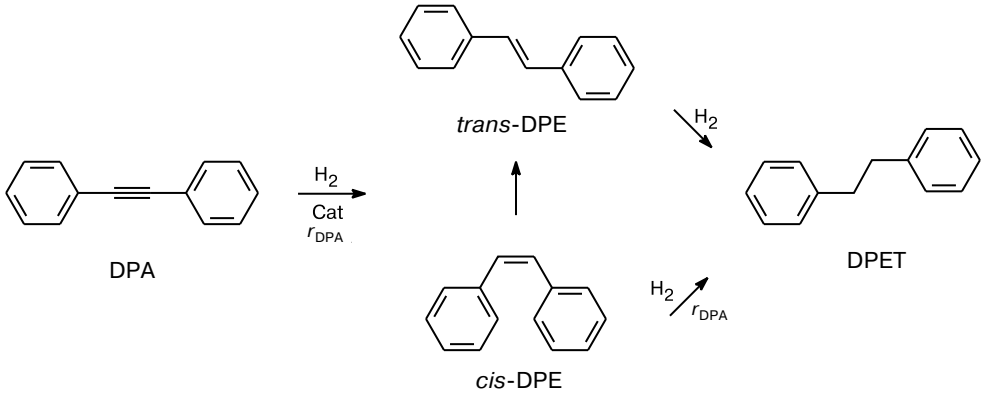

Cat is catalyst, DPE is diphenylethylene, DPET is diphenylethane.

tant characteristic[1] which was carefully controlled in this study.

Experimental

Catalyst preparation. The catalysts Pd(1%)—Cu(1.2%)/Al_2O_3 and Pd(1%)—Cu(1.2%)/SiO_2 were prepared by the incipient wetness impregnation. The supports (γ-Al_2O_3, Sasol, 150 $m^2\ g^{-1}$; SiO_2, Merck, 675 $m^2\ g^{-1}$) were impregnated with a $PdCu_2(AcO)_6$ solution[17] in diluted acetic acid (pH 2.8). The catalysts were dried in air, calcined (air, 550 °C, 2 h) and reduced (H_2(5%)/Ar, 550 °C, 1 h). For the FTIR characterization the samples were prepared with a higher content of the active components (Pd(3%)—Cu(3.6%)).

The monometallic catalysts containing 0.5% Pd and 3% Cu were prepared by the incipient wetness impregnation of the support with an aqueous solution of $[Pd(NH_3)_4](NO_3)_2$ and $Cu(NO_3)_2$ respectively. The samples were dried at ~20 °C and then calcined and reduced under the same conditions as the bimetallic catalysts. For the accurate comparison of the data at close hydrogenation rates, an amount of the active component in monometallic Pd catalysts was diminished to 0.5 wt.% as it is significantly more active in the studied reaction compared to the bimetallic sample.

Hydrogenation of diphenylacetylene (DPA). The liquid phase hydrogenation of DPA was carried out in the autoclave-type reactor equipped with a magnetic stirrer, an electron pressure sensor and gas dosing and liquid phese sampling systems. Commercial *n*-hexane was used as a solvent. The experiments were carried out at 25 °C and initial hydrogen pressure of 10 bar. The kinetic regime was monitored according to the earlier described procedure.[15]

The gas chromatography-mass spectrometer Maestro-2 (Interlab, Russia) was used for the analysis of the reaction mixture. The separation was performed on HP5-MS column (phenyldimethylsiloxane (5%)) of 30 m in length, with the inner diameter of 0.25 mm and thickness 0.25 μm. The gas carrier was helium and an electron beam was used as a method of ionization, 70 eV. The spectra were processed using the MSD ChemStation software and NIST14 spectra library.

The rates of the first and second reaction steps (r_{DPA} and r_{DPE} respectively) were determined from the slope of the curve obtained by plotting hydrogen uptake versus reaction time in the H_2/DPA range from 0.2 to 0.60 for the first step and from 1.1 to 1.5 for the second step and normalized to 1 mg of the catalyst (mmol $H_2\ min^{-1}\ (mg_{cat})^{-1}$).

The catalytic activity was evaluated by the turnover frequencies (TOF). In the case of the bimetallic systems it is hardly possible to determine the number of Pd surface atoms from the electron microscopy data as the surface could be occupied by the copper atoms. For this reason the value of TOF was calculated at the first (TOF_{DPA}) and second (TOF_{DPE}) hydrogenation steps as the ratio of the number of converted substrate (DPA or DPE) molecules to the total number of Pd atoms in the catalyst per second.

The selectivity to diphenylethylene (S_{DPE}) was determined using the data of GC/MS analysis of the reaction mixture:

$$S_{DPE} = n_{DPE}/(n_{DPE} + n_{DPET}).$$

The efficiency of the kinetic process monitoring was estimated by comparing the ratio of the hydrogenation rates of diphenylacetylene (r_{DPA}) and diphenylethylene (r_{DPE}).[13]

Catalyst characterization. *Electron microscopy.* The microstructure of the catalysts was studied by field emission scanning electron microscopy (FE-SEM) on a Hitachi SU8000 microscope. Images were acquired in the secondary electron imaging mode at an accelerating voltage of 2 kV and at a working distance of 4—5 mm. The optimization of the measurements was employed according to the earlier described procedure.[18] Before the measurements, the samples were placed on the surface of a round aluminum holder of 25 mm in diameter, fixed with adhesive tape strips and coated with the conducting metal film (Au/Pd, 60/40) using the the magnetron sputtering method as described elsewhere.[19] The morphology of the samples was studied considering the surface effects of the supported metal film.

IR Spectroscopy of Adsorbed CO. The diffuse reflectance IR spectra of carbon monoxide were recorded on a Protege 460 spectrometer (Nicolet, United States) in the 400—6000 cm^{-1} range at a resolution of 4 cm^{-1}. Carbon monoxide was used as a probe molecule. The sample was placed in a glass vial equipped with an appendix having a calcium ftoride window. Before re-

cording the spectra, the samples were alternately evacuated and treated with H_2 (30 Torr) at 450 °C for 2 h to remove adsorbed gases and water from the surface, as well as for postreduction (heat rate ~3.5 °C min^{-1}). CO adsorbtion was performed at ~20 °C and pressure 20 Torr. CO desorption was carried out under the vacuum with temperature gradually increased from 25 to 100 °C (heating rate ~8 °C min^{-1}) for 1 h until a desired temperature was achieved. The spectra of adsorbed CO were presented as the difference between the spectra recorded before and after adsorption of probe molecule.

Results and Discussion

Electron microscopy. Pd nanoparticles with the mean size of ~2.9 nm are readily seen in the image of the monometallic Pd/Al_2O_3 catalyst (Fig. 1, *a*). When supported on SiO_2 bigger Pd particles are formed with an increased mean particle size close to 3.5 nm (Fig. 1, *b*).

Application of $PdCu_2(AcO)_6$ complex as a metal precursor (Fig. 1, *c*, *d*) increases the metal particle size compared to that in the monometallic catalyst. So, the mean particle size increases to ~4.1 nm in the $Pd—Cu/Al_2O_3$ sample. A similar effect is observed for the $Pd—Cu/SiO_2$ catalyst, which contains the nanoparticles with the mean size of ~5.1 nm.

Catalyst performance. The kinetic plots of the hydrogen uptake *vs*. the reaction time in DPA hydrogenation are shown in Fig. 2. The observed results are in a good agreement with the literature data.[20—22] The form of the curves corresponds to the traditional mechanism of consequent hydrogenation, which is especially evident in a noticeable bend in the range of hydrogen uptakes corresponding to the molar ratio H_2 : DPA = 1. The initial segment of the kinetic curve (H_2/DPA < 1) corresponds to the first hydrogenation step (conversion DPA → DPE). With an increase in the H_2/DPA ratio (>1) hydrogen uptake becomes slower indicating the transition from the first to the second reaction step (conversion DPE → DPET). The calculated kinetic characteristics of the catalysts are presented in Table 1.

Over the monometallic sample Pd/Al_2O_3 the reaction at the first step proceeds with a high rate (r_{DPA} = $= 27.4 \cdot 10^{-3}$ mmol H_2 min^{-1} $(mg_{cat})^{-1}$) which decreases to ~$7.0 \cdot 10^{-3}$ mmol H_2 min^{-1} $(mg_{cat})^{-1}$ at the transition to the second step of hydrogenation. Thus, the rate

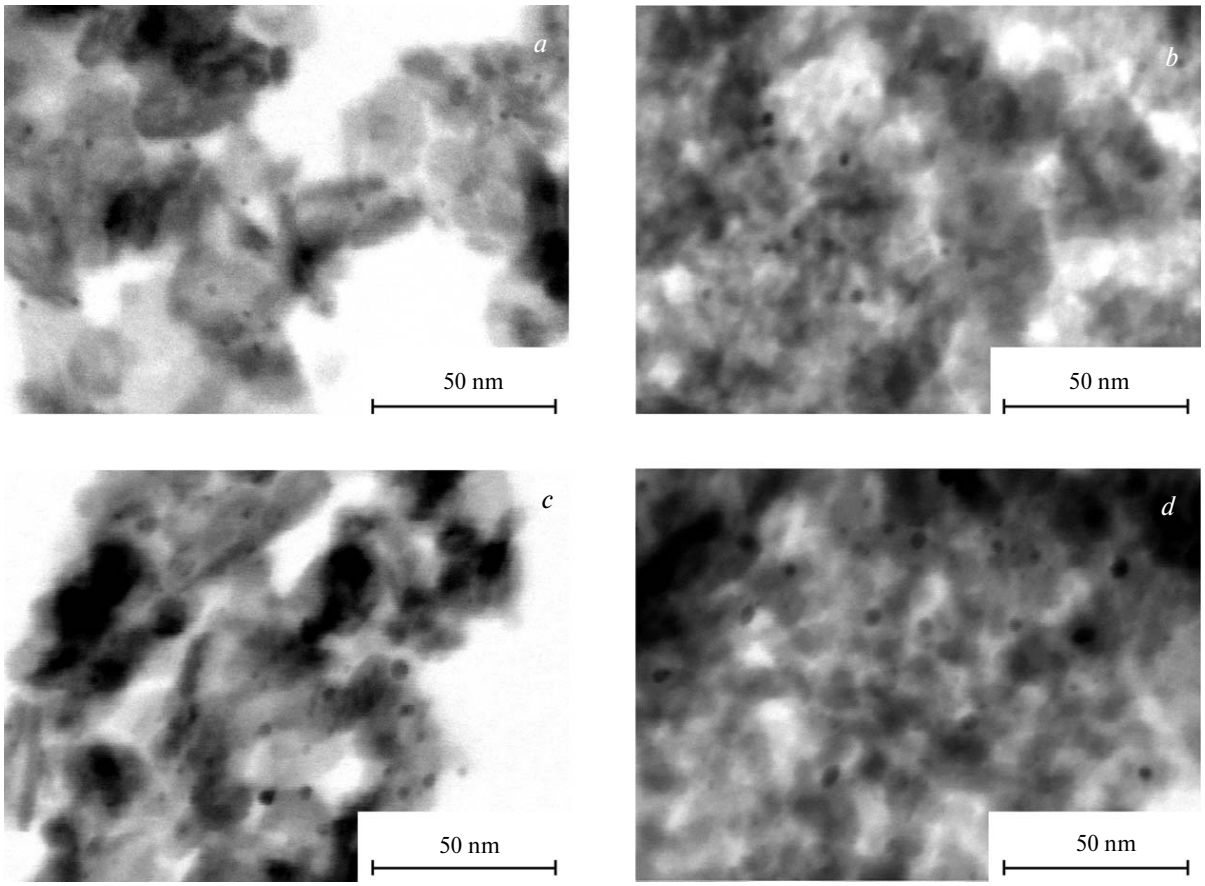

Fig. 1. STEM images for the $Pd(0.5\%)/Al_2O_3$ (*a*), $Pd(0.5\%)/SiO_2$ (*b*), $Pd(1\%)—Cu(1.2\%)/Al_2O_3$ (*c*) and $Pd(1\%)—Cu(1.2\%)/SiO_2$ (*d*) catalysts.

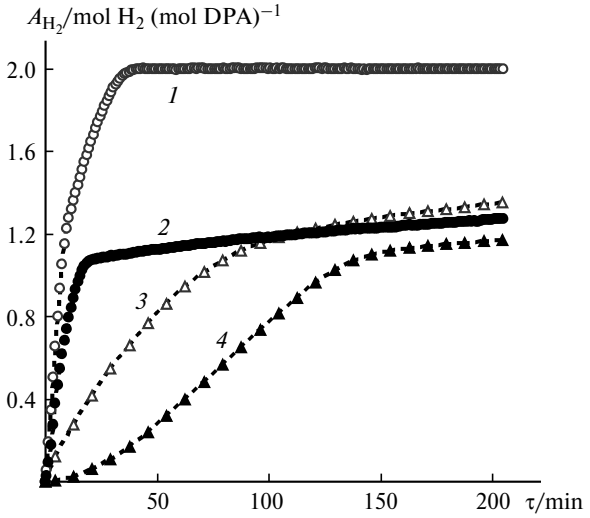

Fig. 2. The kinetic curves of hydrogen uptake in the liquid-phase hydrogenation of DPA over the mono- and bimetallic catalysts: Pd(0.5%)/Al_2O_3 (*1*), Pd(1%)—Cu(1.2%)/Al_2O_3 (*2*), Pd(0.5%)/SiO_2 (*3*), Pd(1%)—Cu(1.2%)/SiO_2 (*4*): $P(H_2)$ = 10 bar, T = 25 °C, [DPA] = 0.159 mol L^{-1}, m_{cat} = 2.5 mg, solvent is *n*-hexane.

ratio r_{DPA}/r_{DPE}, which characterizes the kinetic selectivity is ~3.9.

The rate of the hydrogenation of DPA over Pd/SiO_2 is noticeably lower ($3.09 \cdot 10^{-3}$ mmol H_2 min^{-1} $(mg_{cat})^{-1}$ and on going to the second step it decreases to $0.2 \cdot 10^{-3}$ mmol H_2 min^{-1} $(mg_{cat})^{-1}$, that leads to a rate ratio value of ~15.2. A higher value r_{DPA}/r_{DPE} over Pd/SiO_2 can be partly explained by formation of the large Pd nanoparticles in this sample. In our earlier studies[12,23] it was shown that an increase in Pd nanoparticle size from 2 to 8 nm remarkably increases the ratio r_{DPA}/r_{DPE} in the liquid phase hydrogenation of alkynes.

After the catalyst Pd/Al_2O_3 was modified with copper, the rate of the first step of hydrogenation over Pd—Cu catalyst became somewhat lower than that observed over the monometallic sample. At the second step, reaction rate over Pd—Cu/Al_2O_3 noticeably decreases (from $16.46 \cdot 10^{-3}$ to $0.29 \cdot 10^{-3}$ mmol H_2 min^{-1} $(mg_{cat})^{-1}$). Changing the shape of the kinetic curves can be clearly seen (see Fig. 2) with a visible bend in the range of hydrogen uptake H_2 equal to ~1. In addition, the rate ratio increases 14 times (to ~57).

A decrease in the reaction rate is more pronounced for the Cu containing catalyst supported on SiO_2 than for the catalyst supported on Al_2O_3 (see Fig. 2). The rate values are $1.89 \cdot 10^{-3}$ and $0.07 \cdot 10^{-3}$ mmol H_2 min^{-1} $(mg_{cat})^{-1}$ for the first and the second reaction step correspondingly. As a result, a higher r_{DPA}/r_{DPE} ratio (~26) is observed in comparison with the monometallic Pd/SiO_2 catalyst. The drastic decrease in the reaction rate over Pd—Cu/SiO_2 can be affected by the support nature. Another reason is that bigger bimetallic particles are formed in the Pd—Cu/SiO_2 catalyst than in the Pd—Cu/Al_2O_3 catalyst.

A detailed analysis of the reaction products obtained over the mono- and bimetallic catalysts supported on Al_2O_3 shows that copper introduction remarkably increases the selectivity in formation of the target product of semihydrogenation (Fig. 3). A volcano-type dependence of DPE concentration on the reaction time confirms the consequent mechanism of DPA hydrogenation to DPE followed by DPE conversion to DPET. Over the monometallic catalysts a noticeable amount of DPET (10—15%) is formed at the first reaction step when the concentration of the initial DPA in the reaction mixture is high enough. After the complete conversion of DPA, DPET concentration reaches 25—30% (see Fig. 3, *a*, *c*). Over the bimetallic Pd—Cu catalysts (see Fig. 3, *b*, *d*) the traces of DPET appear only in the range of high DPA conversion and do not exceed 5—8% at the complete DPA hydrogenation. As the DPET formation rate and, consequently, a fraction of the complete hydrogenation products decrease, the maximum yield of DPE increases from 78 to 93% for Pd—Cu/Al_2O_3 and from 78 to 85% for Pd—Cu/SiO_2.

The dependence of selectivity in DPE formation on DPA conversion for the mono- and bimetallic catalyst is shown in Figure 4. It can be seen that by modifying the catalyst with copper it is possible to considerably increase the selectivity of the both Al_2O_3- and SiO_2-supported catalysts. This provides the evidence that the observed effect is nearly independent of the nature of the support. Nevertheless, from the practical point of view, an enhanced selectivity with respect to DPE from 85 to 95% in the region of high DPA conversion can be considered as the most important result.

IR-spectroscopy of the adsorbed CO. The state of the metals in the catalysts was estimated using IR spectra of adsorbed CO (Fig. 5). In the spectra of Pd(0.5%)/Al_2O_3

Table 1. The kinetic characteristics of the mono- and bimetallic catalysts in the selective liquid-phase DPA hydrogenation

Catalyst	$r_{DPA} \cdot 10^3$	$r_{DPE} \cdot 10^3$	TOF_{DPA}	TOF_{DPE}	r_{DPA}/r_{DPE}
	mmol H_2 min^{-1} $(mg_{cat})^{-1}$		s^{-1}		
Pd(0.5%)/Al_2O_3	27.38	6.98	9.71	2.47	3.9
Pd(1%)—Cu(1.2%)/Al_2O_3	16.46	0.29	2.92	0.05	56.6
Pd(0.5%)/SiO_2	3.09	0.2	1.09	0.07	15.2
Pd(1%)—Cu(1.2%)/SiO_2	1.89	0.07	0.33	0.01	26.2

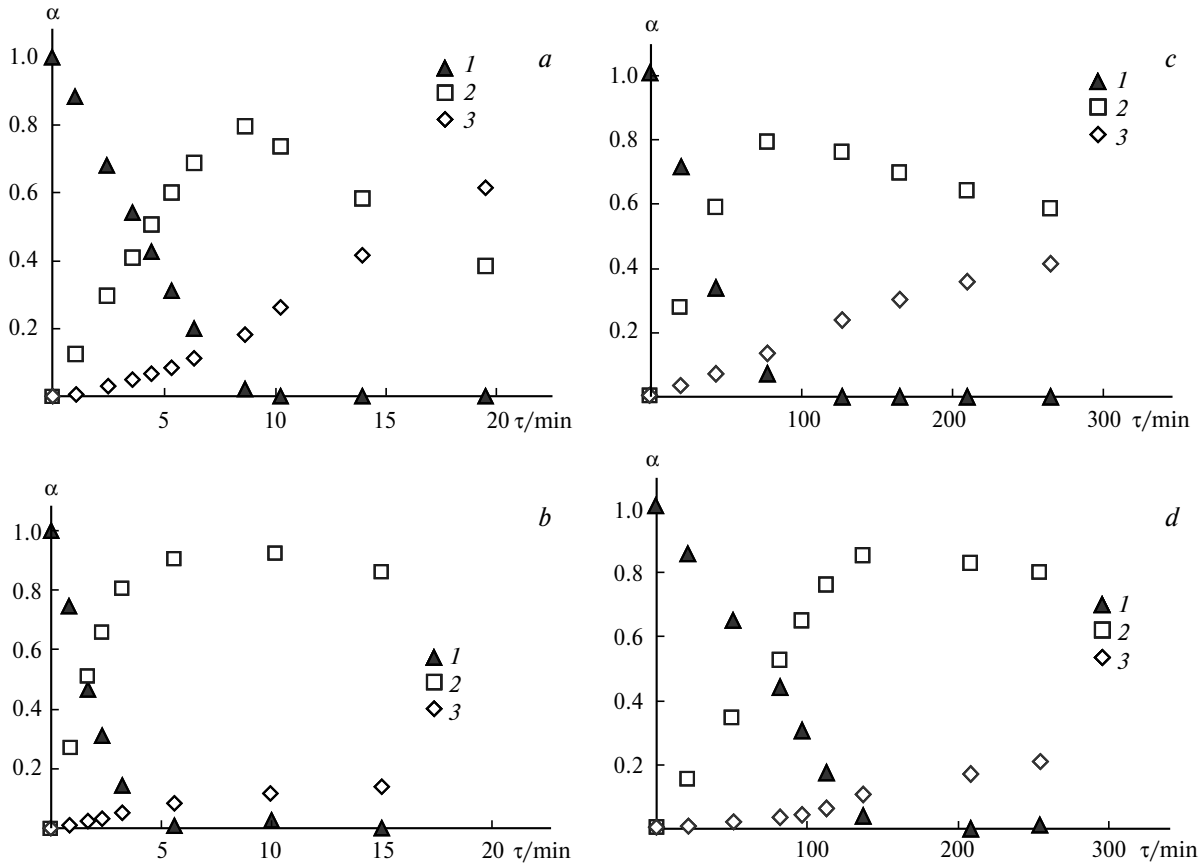

Fig. 3. The reaction mixture composition as a function of the DPA hydrogenation time for the mono- and bimetallic catalysts Pd/Al_2O_3 (*a*), $Pd—Cu/Al_2O_3$ (*b*), Pd/SiO_2 (*c*) and $Pd—Cu/SiO_2$ (*d*): DPA (*1*), DPE (*2*), DPET (*3*); α is mole fraction.

mesured after CO adsorption, the typical bands at 2096 and 1978 cm^{-1} are observed corresponding to the linear forms of CO molecules adsorbed on metallic palladium.[24—29] The band at 2203 cm^{-1} corresponds to CO molecules adsorbed on the low-coordinated cations of the support (Al^{3+}).[24,25] After desorption at ~20 °C the bands due to a bridged form of CO adsorbed on metallic palladium and a linear form of CO adsorbed on alumina cations disappear. Moreover, the band of the liner form of CO adsorption shifts towards lower frequencies resulting from the absence of the dipole-dipole interaction of the nearby adsorbed CO molecules («red» shift). The position of the Pd^0—CO singlenton in IR spectra corresponds to 2068 cm^{-1}. An increase in desorption temperature to 100 °C leads to a complete disappearance of this band.

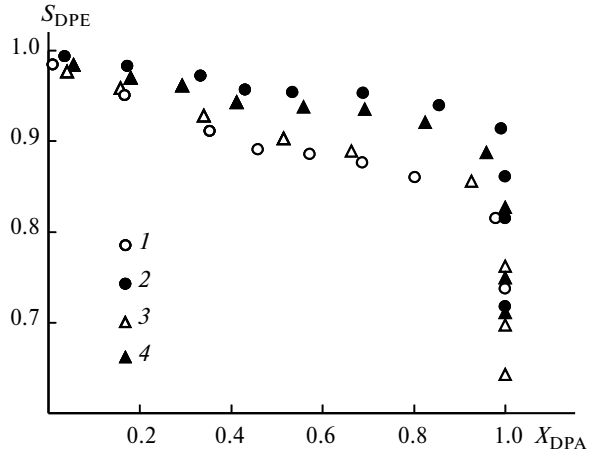

Fig. 4. The dependence of selectivity to DPE formation (S_{DPE}) on DPA conversion (X_{DPA}) for the mono- and bimetallic catalysts in the selective DPA hydrogenation: $Pd(0.5\%)/Al_2O_3$ (*1*), $Pd(1\%)—Cu(1.2\%)/Al_2O_3$ (*2*), $Pd(0.5\%)/SiO_2$ (*3*), $Pd(1\%)—Cu(1.2\%)/SiO_2$ (*4*): $P(H_2)$ = 10 bar, T = 25 °C, [DPA] = = 0.159 mol L^{-1}, m_{cat} = 2.5 mg, solvent is *n*-hexane.

The spectrum of CO adsorbed on $Cu(3\%)/Al_2O_3$, includes a strong asymmetric band with a maximum at 2143 cm^{-1} corresponding to stretching vibrations of CO molecule adsorbed on Cu^+ cations in linear form.[24—31] The asymmetry of this band can be attributed to the presence of different copper sites, such as Cu^+ and unreduced Cu^{2+}, characterized by a small discrepancy in the energy. Desorption at ~20 °C decreases the intensity while further desorption at 100 °C removes this band. Only a weak band at 2126 cm^{-1} persist. The presence of this band appears to affect the symmetry of the main band observed after ad-

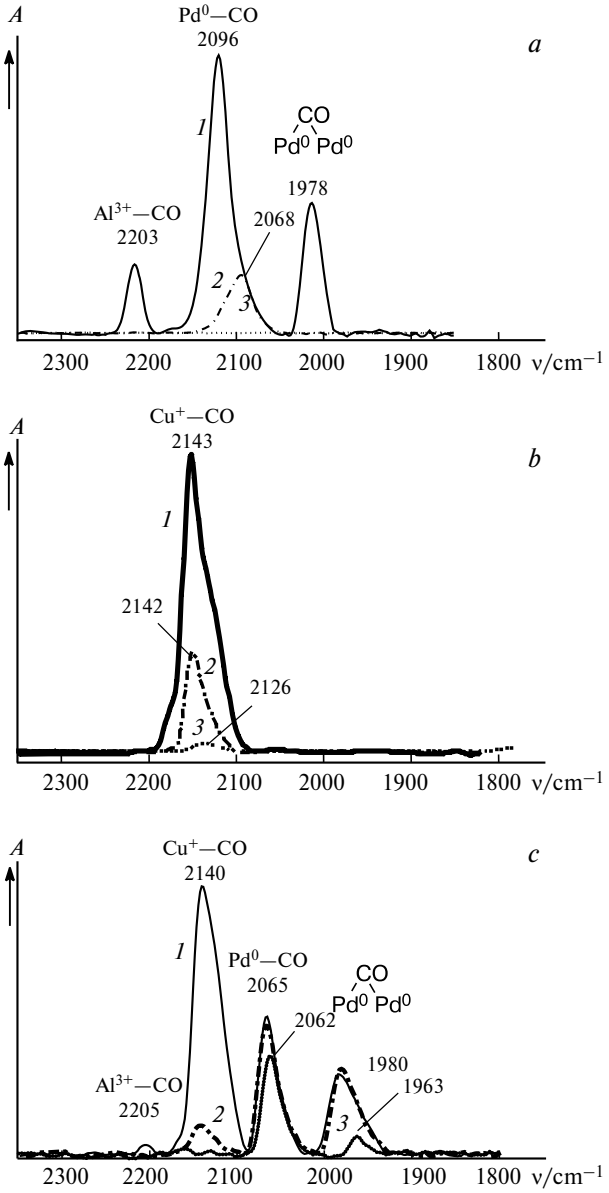

Fig. 5. FTIR-spectra of CO adsorbed at ~20 °C on the Pd(0.5%)/Al_2O_3 (*a*), Cu(3%)/Al_2O_3 (*b*) and Pd(3%)—Cu(3.6%)/Al_2O_3 (*c*) catalysts: adsorption (*1*), desorption at 25 (*2*) and at 100 °C (*3*).

sorption of CO because CO molecules are more tightly bound by Cu^+ sites. No bands characterizing CO adsorption on Cu^0-centers are observed, which gives evidence to a low stability of the CO—Cu^0 complexes.[24,25]

The IR spectrum of CO adsorbed on Pd(3%)—Cu(3.6%) includes four adsorption bands. The weak band at 2205 cm^{-1}, attributable to the carbonyl Al^{3+}—CO complex, completely disappears after removal of the gas phase. The symmetric band at 2140 cm^{-1} relates to the stretching vibrations of CO molecules adsorbed on Cu^+ cations. The following evacuation almost removes this band. The intensities of the bands at 2065 and 1980 cm^{-1}, which characterize the linear and bridged forms of CO adsorption on Pd^0 correspondingly, remain unchanged after evacuation at ~20 °C. An increase in the desorption temperature to 100 °C has a slight effect on the position and intensity of the band at 2065 cm^{-1}. That can be a proof of the formation of Pd—Cu alloy particles in the bimetallic catalyst. After the evacuation at 100 °C the intensity of the band at 1980 cm^{-1} increases considerably with a maximum shifted to 1965 cm^{-1}. An additional argument in favour of the formation of bimetallic alloy in the Pd(3%)—Cu(3.6%) sample can be the change in the ratio between the linear and bridged CO—Pd^0 forms when compared with the monometallic sample.

Thus, we showed that by modifying the catalyst with copper it is possible to noticeably decrease the reaction rate of the second step and increases the ratio r_{DPA}/r_{DPE}. Some decrease in the activity of the bimetallic catalyst dramatically increases the selectivity of the target product of semihydrogenation (DPE) from 85 to 95% at high conversion of DPA (90—95%). Such behaviour can be explained by the formation of bimetallic Pd—Cu nanoparticles resulted from the reduction of heterobimetallic $PdCu_2(AcO)_6$ complex. Since Pd—Cu alloy is formed, an amount of Pd active atoms decreases as well as the heat of semihydrogenated alkene adsorption facilitating its desorption and reducing the probability of the ensuing hydrogenation to alkane. As a result, a decrease in the rate of the second step of the process and respectively an increase in the selectivity, are observed.[9] The formation of bimetallic particles was proved by both the FTIR-CO and electron microscopy.

The authors are grateful to the Department of the Structure Study of ZIOC RAS (Moscow) for the characterization of the samples by electron microscopy and the International Analytical Centre of ZIOC RAS for the given opportunity to analyse reaction products by CG/MS technique.

This work was financially supported by the Russian Foundation for Basic Research (Project No. 13-03-121761_ofi_m).

References

1. H. U. Blaser, A. Schnyder, H. Steiner, F. Rossler, P. Baumeister, in *Handbook of Heterogeneous Catalysis*, Eds G. Ertl, H. Knözinger, F. Schüth, J. Weitkamp, Wiley-VCH Verlag GmbH&Co. KGaA, Weinheim, Germany, 2008, vol. **8**, p. 3298.
2. V. P. Ananikov, L. L. Khemchyan, Yu. V. Ivanova, V. I. Bukhtiyarov, A. M. Sorokin, I. P. Prosvirin, S. Z. Vatsadze, A. V. Medved´ko, V. N. Nuriev, A. D. Dilman, V. V. Levin, I. V. Koptyug, K. V. Kovtunov, V. V. Zhivonitko, V. A. Likholobov, A. V. Romanenko, P. A. Simonov, V. G. Nenajdenko, O. I. Shmatova, V. M. Muzalevskiy, M. S. Nechaev, A. F. Asachenko, O. S. Morozov, P. B. Dzhevakov, S. N.

Osipov, D. V. Vorobyeva, M. A. Topchiy, M. A. Zotova, S. A. Ponomarenko, O. V. Borshchev, Yu. N. Luponosov, A. A. Rempel, A. A. Valeeva, A. Yu. Stakheev, O. V. Turova, I. S. Mashkovsky, S. V. Sysolyatin, V. V. Malykhin, G. A. Bukhtiyarova, A. O. Terent´ev, I. B. Krylov, *Russ. Chem. Rev.*, 2014, **83**, 885.
3. V. P. Ananikov, E. A. Khokhlova, M. P. Egorov, A. M. Sakharov, S. G. Zlotin, A. V. Kucherov, L. M. Kustov, M. L. Gening, N. E. Nifantiev, *Mendeleev Commun.*, 2015, **25**, 75.
4. A. Borodzinski, G. C. Bond, *Catal. Rev.*, 2006, **48**, 91.
5. K. R. Campos, D. Cai, M. Journet, J. J. Kowal, R. D. Larsen, P. J. Reider, *J. Org. Chem.*, 2001, **66**, 3634.
6. G. C. Bond, in *Metal-Catalysed Reactions of Hydrocarbons*, Springer Science + Business Media, Inc., New York, 2005, p. 395.
7. N. A. Khan, S. Shaikhutdinov, H.-J. Freund, *Catal. Lett.*, 2006, **108**, 159.
8. A. A. Lamberov, S. R. Egorova, I. R. Il´yasov, Kh. Kh. Gil´manov, S. V. Trifonov, V. M. Shatilov, Sh. Ziyatdinov, *Kinet. Catal.* (*Int. Ed.*), 2007, **48**, 136 [*Kinetika i Kataliz*, 2007, **48**, 143].
9. I. S. Mashkovskii, O. P. Tkachenko, G. N. Baeva, A. Yu. Stakheev, *Kinet. Catal.* (*Int. Ed.*), 2009, **50**, 768 [*Kinetika i Kataliz*, 2009, **50**, 798].
10. I. S. Mashkovsky, G. N. Baeva, A. Yu. Stakheev, M. N. Vargaftik, N. Yu. Kozitsyna, I. I. Moiseev, *Mendeleev Commun.*, 2014, **24**, 355.
11. T. V. Choudhary, C. Sivadinarayana, A. K. Datye, D. Kumar, D. W. Goodman, *Catal. Lett.*, 2003, **86**, 1.
12. A. Yu. Stakheev, B. L. Moroz, I. S. Mashkovsky, P. V. Markov, O. V. Turova, O. P. Tkachenko, P. A. Pyryaev, V. I. Bukhtiyarov, *Russ. Chem. Bull.* (*Int. Ed.*), 2015, **64**, 53 [*Izv. Akad. Nauk, Ser. Khim.*, 2015, 53].
13. M. P. R. Spee, J. Boersma, M. D. Meijer, M. Q. Slagt, G. van Koten, J. W. Geus, *J.Org. Chem.*, 2001, **66**, 1647.
14. L. Guczi, Z. Schay, Gy. Stefler, L. F. Liotta, G. Deganello, A. M. Venezia, *J. Catal.*, 1999, **182**, 456.
15. P. V. Markov, G. O. Bragina, G. N. Baeva, O. P. Tkachenko, I. S. Mashkovsky, I. A. Yakushev, N. Yu. Kozitsyna, M. N. Vargaftik, A. Yu. Stakheev, *Kinet. Catal.* (*Int. Ed.*), 2015, **56**, 591 [*Kinetika i Kataliz*, 2015, **56**, 599].
16. O. P. Tkachenko, A. Yu. Stakheev, L. M. Kustov, I. S. Mashkovsky, M. van den Berg, W. Grünert, N. Yu. Kozitsyna, S. E. Nefedov, Zh. V. Dobrokhotova, V. I. Zhilov, M. N. Vargaftik, I. I. Moiseev, *Catal. Lett.*, 2006, **112**, 155.
17. N. Yu. Kozitsyna, S. E. Nefedov, F. M. Dolgushin, N. V. Cherkashina, M. N. Vargaftik, I. I. Moiseev, *Inorg. Chim. Acta*, 2006, **359**, 2072.
18. V. V. Kachala, L. L. Khemchyan, A. S. Kashin, N. V. Orlov, A. A. Grachev, S. S. Zalesskiy, V. P. Ananikov, *Russ. Chem. Rev.*, 2013, **82**, 648.
19. A. S. Kashin, V. P. Ananikov, *Russ. Chem. Bull.* (*Int. Ed.*), 2011, **60**, 2602 [*Izv. Akad. Nauk, Ser. Khim.*, 2011, 2551].
20. N. Marin-Astorga, G. Alvez-Manoli, P. Reyes, *J. Mol. Catal. A Chem.*, 2005, **226**, 81.
21. B. M. Choudary, M. Lakshmi Kantam, N. Mahender Reddy, K. Koteswara Rao, Y. Haritha, V. Bhaskar, F. Figueras, A. Tuel, *Appl. Catal. A*, 1999, **181**, 139.
22. X.-Y. Quek, Y. Guan, E. J. M. Hensen, *Catal. Today*, 2012, **183**, 72.
23. A. Yu. Stakheev, P. V. Markov, A. S. Taranenko, G. O. Bragina, G. N. Baeva, O. P. Tkachenko, I. S. Mashkovsky, A. S. Kashin, *Kinet. Catal.* (*Ind. Ed.*), 2015, **56**, 733 [*Kinetika i Katal.*, 2015, **56**, 721].
24. A. Davidov, in *Molecular Spectroscopy of Oxide Catalyst Surfaces*, Wiley, New York, 2003, 691 pp.
25. K. I. Hadjiivanov, G. N. Vayssilov, *Adv. Catal.*, 2002, **47**, 307.
26. S. Sitthisa, T. Pham, T. Prasomsri, T. Sooknoi, R. G. Mallinson, D. E. Resasco, *J. Catal.*, 2011, **280**, 17.
27. B. T. Meshesha, N. Barrabes, J. Llorca, A. Dafinov, F. Medina, K. Föttinger, *Appl. Catal. A: General*, 2013, **453**, 130.
28. P. Benito, M. Gregori, S. Andreoli, G. Fornasari, F. Ospitali, S. Millefanti, M. S. Avila, T. F. Garett, S. Albonetti, *Catal. Today*, 2015, **246**, 108.
29. M. Fernandez-Garcia, A. Martinez-Arias, A. Iglesias-Juez, A. B. Hungria, J. A. Anderson, J. C. Conesa, J. Soria, *Appl. Catal. B: Environmental*, 2001, **31**, 39.
30. A. B. Hungria, A. Iglesias-Juez, A. Martinez-Arias, M. Fernandez-Garcia, J. A. Anderson, J. C. Conesa, J. Soria, *J. Catal.*, 2002, **206**, 281.
31. V. Yu. Borovkov, D. R. Luebke, V. I. Kovalchuk, J. L. d´Itri, *J. Phys. Chem. B*, 2003, **107**, 5568.

Received November 16, 2015;
in revised form November 25, 2015